Hydrodynamic Interactions of Waves with Group of Truncated Vertical Cylinders

By Oguz Yılmaz[1]

Abstract: An exact analytical method is described to solve the diffraction and radiation problems of a group of truncated vertical cylinders. In order to account for the interaction between the cylinders, Kagemoto and Yue's exact algebraic method is utilized. The isolated cylinder diffraction and radiation potentials are obtained using Garret's solution, and evanescent mode solutions are derived in a similar manner. Numerical results are presented for arrays of two and four cylinders. Comparisons between the results obtained from the method presented here and those obtained from numerical methods show excellent agreement.

INTRODUCTION

The phenomenon of hydrodynamic interaction among cylinders in a group, for example between the columns of tension leg platforms (TLPs) or semisubmersibles, has received considerable interest in recent years. Although numerical calculations through the use of Green's function techniques are well established, their use may be expensive and cumbersome. An alternative method is to obtain semianalytical solutions that take the hydrodynamic interactions into account. Linton and Evans (1990) improved on Spring and Monkmeyer's (1974) direct matrix method, wherein the amplitudes of the wave components around each body are solved simultaneously, to obtain simple expressions for force and free surface amplitudes. Another approach to the problem is the multiple scattering technique (Ohkusu 1974), in which successive scatters by each of the cylinders are introduced at each order. Kagemoto and Yue (1986) combined the direct matrix method and the multiple scattering technique to obtain an exact algebraic method. In their interaction theory, the scattered wave field around each body is expressed as a summation of cylindrical waves with undetermined amplitudes. By using addition theorems for Bessel functions, the scattered potential at one body is evaluated in the coordinate systems of other bodies. A set of linear algebraic equations that relates the total incident potential to the scattered potential is then solved simultaneously for all the unknown amplitude coefficients. Kim (1992) reviewed the diffraction theory of Linton and Evans (1990) and extended it to the radiation problem.

However, some researchers used a large-spacing approximation to solve the problem, ignoring the evanescent waves. Simon (1982) developed a plane wave approximation in a direct matrix solution of a uniformly spaced linear array of axisymmetric bodies. In this method, the diverging waves at one body due to the scattering of another body are replaced by a single wave plane. Errors introduced are not significant, and computational time is reduced significantly. Simon applied his method to the heaving motion of axisymmetric bodies only. McIver and Evans (1984) extended Simon's approach to the study of wave forces on arrays of fixed vertical circular cylinder by including a correction term in the plane wave approximation. They obtained significantly improved results, even when the body spacings are fairly small compared with the wavelength. McIver (1984) extended this method to the calculation of added mass and damping. Williams and Demirbilek (1988) used the modified plane wave method of McIver and Evans to calculate the diffraction forces between the members of an array of stationary truncated circular cylinders of equal radius. Williams and Abul-Azm (1989) extended their method to calculate added mass and damping, using McIver's method. By using the same approach, Williams and Rangappa (1994) calculated hydrodynamic loads and added mass and damping coefficients for multicolumn offshore platforms consisting of arrays of semiimmersed or submerged cylindrical structures.

In this paper Kagemoto and Yue's (1986) interaction theory is used to obtain analytical solutions for the diffraction and radiation problem of truncated cylinders. The diffraction and radiation potentials of an isolated cylinder are obtained using Garret's (1971) solution, and evanescent mode solutions are derived in a similar manner to Garret's (1971) solution. Numerical results are presented for arrays of four cylinders. Comparisons between the results obtained from the method presented in this paper and those obtained from numerical methods are excellent.

THEORETICAL DEVELOPMENT

Diffraction Problem

An array of N truncated cylinders of equal radius a are placed in water of uniform depth d. The clearance beneath each cylinder is denoted by h. Used here are $N + 1$ coordinate systems: (r, θ, z) with the origin at the seabed and the z-axis positive upward. Local coordinates (r_i, θ_i, z), $i = 1, \ldots, N$ centered at the origin of each cylinder (x_i, y_i) are also used. The coordinate systems and the parameters used are depicted in Fig. 1.

Assuming that the fluid is ideal and waves are of small amplitude, the fluid motion may be described by a velocity potential $\phi(x, y, z, t) = \mathrm{Re}\{\varphi(x, y, z)e^{-i\omega t}\}$. This potential must satisfy Laplace's equation together with boundary conditions at the free surface, on the body, and at the sea bottom, and a suitable radiation condition for the diffraction potential at infinity.

An incident wave potential for a plane wave of amplitude H, frequency ω, and wave heading angle β has the following form:

$$\varphi_{0j} = \frac{gH}{\omega} Y_0(z) I_j e^{ik_0 r_j \cos(\theta_j - \beta)} \tag{1a}$$

$$\varphi_{0j} = \frac{gH}{\omega} Y_0(z) I_j \sum_{n=-\infty}^{\infty} e^{in[(\pi/2)-\theta_j+\beta]} J_n(k_0 r_j) \tag{1b}$$

where $I_j = e^{ik_0(x_j \cos\beta + y_j \sin\beta)}$ = phase factor associated with cylinder j; and $i = \sqrt{-1}$. Wave number k_0 and frequency ω satisfy the dispersion relationship $\omega^2 = k_0 g \tanh k_0 d$ with g being gravitational acceleration. J_n is the first kind of Bessel function of order n.

[1]Assoc. Prof., Istanbul Tech. Univ., Facu. of Naval Arch. and Oc. Engrg., Maslak, Istanbul, Turkey.

Note. Discussion open until March 1, 1999. To extend the closing date one month, a written request must be filed with the ASCE Manager of Journals. The manuscript for this paper was submitted for review and possible publication on September 30, 1996. This paper is part of the ***Journal of Waterway, Port, Coastal, and Ocean Engineering***, Vol. 124, No. 5, September/October, 1998. ©ASCE, ISSN 0733-950X/98/0005-0272–0279/$8.00 + $.50 per page. Paper No. 14303.

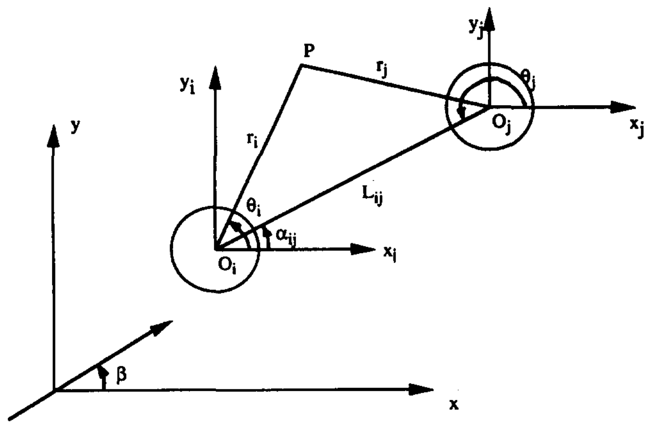

FIG. 1. Plan View of Two Cylinders and Coordinate Systems

$$Y_0(z) = \frac{\cosh(k_0 z)}{\cosh(k_0 d)} \quad \text{for} \quad m = 0 \tag{2a}$$

$$Y_m(z) = \cos(k_m z) \quad \text{for} \quad m > 0 \tag{2b}$$

By replacing n with $-n$, (1) is rewritten as follows:

$$\varphi_{0j} = \frac{gH}{\omega} Y_0(z) \sum_{n=-\infty}^{\infty} \mathbf{a}_j^I(n)\psi_j^I(n) \tag{3}$$

where $\mathbf{a}_j^I(n) = I_j e^{in[(\pi/2)-\beta]}$ and $\psi_j^I(n) = J_n(k_0 r_j)e^{in\theta_j}$.

The general form of scattered wave field outside the immediate neighborhood of body i can be expressed as a summation of cylindrical waves as follows:

$$\varphi_i^S = \frac{gH}{\omega}\left[Y_0(z)\sum_{n=-\infty}^{\infty} A_{on_i} H_n^{(1)}(k_0 r_i)e^{in\theta_i} + \sum_{m=1}^{\infty} Y_m(z) \sum_{n=-\infty}^{\infty} A_{mn_i} K_n(k_m r_i) e^{in\theta_i}\right] \tag{4}$$

where $H_n^{(1)}$ and K_n = nth-order Hankel function of the first kind and modified Bessel function of the second kind, respectively; and the wave number k_m ($m = 1, 2, \ldots$) = positive real root of the dispersion equation $\omega^2 = -k_m g \tan k_m d$. The condition $m > 0$ corresponds to the evanescent modes.

In order to express the scattered potential in the other cylinders' coordinate systems, addition theorems for Bessel functions (Abramowitz and Stegun 1964) will be used:

$$H_n^{(1)}(k_0 r_i)e^{in\theta_i} = \sum_{l=-\infty}^{\infty} H_{n+l}^{(1)}(k_0 L_{ij}) J_l(k_0 r_j) e^{i\alpha_{ij}(l+n)} e^{il(\pi-\theta_j)} \tag{5a}$$

$$K_n(k_m r_i)e^{in\theta_i} = \sum_{l=-\infty}^{\infty} K_{n+l}(k_m L_{ij}) I_l(k_m r_j) e^{i\alpha_{ij}(l+n)} e^{il(\pi-\theta_j)} \tag{5b}$$

where I_l = lth-order modified Bessel function of the first order.

By substituting (5*a*) and (5*b*) in (4) and replacing l by $-l$, one obtains

$$\varphi_i^S = \frac{gH}{\omega}\left[Y_0(z)\sum_{n=-\infty}^{\infty} A_{on_i} \sum_{l=-\infty}^{\infty} H_{n-l}^{(1)}(k_0 L_{ij}) e^{i\alpha_{ij}(n-l)} J_l(k_0 r_j) e^{il\theta_j} + \sum_{m=1}^{\infty} Y_m(z) \sum_{n=-\infty}^{\infty} A_{mn_i} \sum_{l=-\infty}^{\infty} K_{n-l}(k_m L_{ij}) e^{i\alpha_{ij}(n-l)}(-1)^l I_l(k_m r_j) e^{il\theta_j}\right] \tag{6}$$

Eq. (6) can be written in matrix notation as follows:

$$\varphi_i^S = \frac{gH}{\omega}[Y_0(z)\mathbf{A}_i^T(n)\mathbf{T}_{ij}(n, l)\psi_j^I(l) + Y_m(z)\mathbf{A}_i^T(m, n)\mathbf{T}_{ij}(m, n, l)\psi_j^I(m, l)] \tag{7}$$

where

$$\mathbf{T}_{ij}(n, l) = H_{n-l}^{(1)}(k_0 L_{ij}) e^{i\alpha_{ij}(n-l)}$$

$$\text{and} \quad \psi_j^I(l) = J_l(k_0 r_j)e^{il\theta_j} \quad \text{for} \quad m = 0 \tag{8a}$$

$$\mathbf{T}_{ij}(m, n, l) = K_{n-l}(k_m L_{ij}) e^{i\alpha_{ij}(n-l)}(-1)^l$$

$$\text{and} \quad \psi_j^I(m, l) = I_l(k_m r_j)e^{il\theta_j} \quad \text{for} \quad m > 0 \tag{8b}$$

The total incident velocity potential near body j is the summation of the ambient incident wave field and the scattered wave field due to other cylinders:

$$\varphi_j^I = \varphi_{0j} + \sum_{\substack{i=1 \\ (i \neq j)}}^{N} \mathbf{A}_i^T \mathbf{T}_{ij} \psi_j^I; \quad \varphi_j^I = \left(\mathbf{a}_j^T + \sum_{\substack{i=1 \\ (i \neq j)}}^{N} \mathbf{A}_i^T \mathbf{T}_{ij}\right)\psi_j^I \tag{9a,b}$$

According to Kagemoto and Yue (1986), the total incident and scattered waves for any body j are related to each other by the isolated body diffraction characteristics of that body, which will be denoted by $\mathbf{B}_j$ ($j = 1, 2, \ldots, N$):

$$\mathbf{A}_j(n) = \mathbf{B}_j(n, l)\left[\mathbf{a}_j(l) + \sum_{\substack{i=1 \\ (i \neq j)}}^{N} \mathbf{T}_{ij}^T(n, l)\mathbf{A}_i(n)\right] \quad \text{for} \quad m = 0 \tag{10}$$

A similar equation can be written for $m > 0$. Single body diffraction matrices $\mathbf{B}_j$ are obtained by solving the diffraction problem of a truncated cylinder including both progressive and evanescent modes. These solutions are given in Appendix I, and $\mathbf{B}_j$ is given as follows:

$$\mathbf{B}_j(n, l) = -\frac{J_l'(k_0 a)}{H_l'(k_0 a)} + \frac{D_0^{(l)} \cosh(k_0 d)}{H_l'(k_0 a) N_0^{1/2}} \quad \text{for} \quad m = 0 \tag{11a}$$

$$\mathbf{B}_j(m, n, l) = -\frac{I_l'(k_m a)}{K_l'(k_m a)} + \frac{D_m^{(l)}}{K_l'(k_m a) N_m^{1/2}} \quad \text{for} \quad m > 0 \tag{11b}$$

where

$$N_0 = \frac{1}{2}\left(1 + \frac{\sinh 2k_0 d}{2k_0 d}\right) \quad \text{and} \quad N_m = \frac{1}{2}\left(1 + \frac{\sin 2k_m d}{2k_m d}\right) \tag{12}$$

Once $\mathbf{B}_j$ is determined, $\mathbf{A}_j$ can be obtained from (10) and first-order forces can be evaluated by integrating the total potential on the cylinder. The surge force on cylinder j is calculated as follows:

$$F_{x_j} = -i\rho g H \int_{\theta=0}^{2\pi}\int_{z=h}^{d}\left[\left(\mathbf{a}_j^T + \sum_{\substack{i=1 \\ (i \neq j)}}^{N} \mathbf{A}_i^T \mathbf{T}_{ij}\right)\mathbf{B}_j^T \psi_j^S(a, \theta_j) Y_m(z) + \left(\mathbf{a}_j^T + \sum_{\substack{i=1 \\ (i \neq j)}}^{N} \mathbf{A}_i^T \mathbf{T}_{ij}\right)\psi_j^I(a, \theta_j) Y_m(z)\right] a \cos\theta_j \, d\theta_j \, dz \quad (m \geq 0) \tag{13}$$

where $\psi_j^S = H_l^{(1)}(k_0 r_j)e^{il\theta_j}$ for $m = 0$; and $\psi_j^S = K_l(k_m r_j)e^{il\theta_j}$ for $m > 0$.

The first term in (13) is due to the diffraction effects; the second is due to the ambient incident field and scattering of all the other bodies. The heave force is evaluated in a similar manner, but the $\mathbf{B}_j$ matrix used in the heave force calculation is different from the one used in the interaction theory and is given as follows:

$$\mathbf{B}_{hj}(n, l) = \frac{C_0^{(l)}}{2a^l} \quad \text{for} \quad m = 0 \tag{14a}$$

$$\mathbf{B}_{hj}(m, n, l) = \frac{C_m^{(l)}}{I_l\left(\frac{m\pi a}{h}\right)}(-1)^m \quad \text{for} \quad m > 0 \tag{14b}$$

The derivation of these matrices is given in Appendix I.

In addition to this, the incident wave potential must be subtracted from the first term and integrated since the interior region potential obtained from the single body diffraction solution contains both incident and scattered wave fields:

$$F_{z_j} = i\rho g H \int_{\theta=0}^{2\pi} \int_{r=0}^{a} \left[\left(\mathbf{a}_j^T + \sum_{\substack{i=1 \\ (i \neq j)}}^{N} \mathbf{A}_i^T \mathbf{T}_{ij} \right) \mathbf{B}_{hj}^T \boldsymbol{\psi}_j^S(r_j, \theta_j) \right.$$

$$+ \left(\mathbf{a}_j^T + \sum_{\substack{i=1 \\ (i \neq j)}}^{N} \mathbf{A}_i^T \mathbf{T}_{ij} \right) \boldsymbol{\psi}_j^I(r_j, \theta_j) Y_m(h)$$

$$\left. - \left(\mathbf{a}_j^T + \sum_{\substack{i=1 \\ (i \neq j)}}^{N} \mathbf{A}_i^T \mathbf{T}_{ij} \right) Y_m(h) i^l J_l(k_0 r_j) e^{il\theta_j} \right] r_j \, d\theta_j \, dr_j \quad (m \geq 0) \tag{15}$$

where $\psi_j^S = r_j^{|l|} e^{il\theta_j}$ for $m = 0$; and $\psi_j^S = I_l(m\pi r/h) e^{il\theta_j}$ for $m > 0$.

Pitch moment is calculated about an axis that is parallel to the y-axis and passes through the geometrical center of the bodies on the still water plane. The shortest distance between the bodies and the pitch rotation axis is denoted as X_i ($i = 1, \ldots, N$). Therefore the pitch moment arising from the heave forces can be calculated by taking the moments of the forces about the axis, i.e., the integrand in (15) is multiplied by the lever ($X_i - r_i \cos \theta$). To calculate the pitch moment arising from the surge forces, the integrand in (13) is multiplied by the lever ($d - z$). Summation of the two components gives the total pitch moment.

Integrals in (13), (15), and their modified forms used to calculate the pitch moment are very easy to evaluate, and the details will not be given here.

Radiation Problem

Formulation of the problem follows closely that of the diffraction problem. Radiated waves will replace the incident waves, therefore (10) is rewritten as follows:

$$\mathbf{A}_j(n) = \mathbf{B}_j(n, l) \left[\sum_{\substack{i=1 \\ (i \neq j)}}^{N} \mathbf{T}_{ij}^T(n, l) \mathbf{R}_i(n, l) + \sum_{\substack{i=1 \\ (i \neq j)}}^{N} \mathbf{T}_{ij}^T(n, l) \mathbf{A}_i(n) \right] \tag{16}$$

where $\mathbf{R}_i(n, l)$ = single body radiation characteristics. For heave motion $\mathbf{R}_i(n, l)$ exists for $l = 0$ only and is given by

$$\mathbf{R}_i(0, 0) = D_0 \frac{\cosh k_0 d}{N_0^{1/2} H_0^{(1)'}(k_0 a)} \quad \text{for} \quad m = 0 \tag{17a}$$

$$\mathbf{R}_i(m, n, 0) = \frac{D_n}{N_n^{1/2} K_0'(k_n a)} \quad \text{for} \quad m > 0 \tag{17b}$$

As for the surge motion, there are two modes to be considered, $l = -1$ and $l = 1$:

$$\mathbf{R}_i(0, -1) = -D_0 \frac{\cosh k_0 d}{2 N_0^{1/2} H_1^{(1)'}(k_0 a)}$$

$$\text{and} \quad \mathbf{R}_i(0, 1) = D_0 \frac{\cosh k_0 d}{2 N_0^{1/2} H_1^{(1)'}(k_0 a)} \quad \text{for} \quad m = 0 \tag{18a}$$

$$\mathbf{R}_i(m, n, -1) = \frac{D_n}{2 N_n^{1/2} K_1'(k_n a)} \quad \text{and} \quad \mathbf{R}_i(m, n, 1) = \frac{D_n}{2 N_n^{1/2} K_1'(k_n a)}$$

$$\text{for} \quad m > 0 \tag{18b}$$

These matrices are derived from (55) and (67).

Once $\mathbf{B}_j$ and $\mathbf{R}_i$ are determined, $\mathbf{A}_j$ can be obtained from (16) and added mass and damping coefficients can be evaluated by integrating the total potential around the cylinder. The surge and heave added mass and damping coefficients of cylinder j are calculated as follows:

$$a_{xx_j} + i \frac{b_{xx_j}}{\omega} = -\rho d \int_{\theta=0}^{2\pi} \int_{z=h}^{d} \left[\left(\mathbf{a}_j^T + \sum_{\substack{i=1 \\ (i \neq j)}}^{N} \mathbf{A}_i^T \mathbf{T}_{ij} \right) \mathbf{B}_j^T \boldsymbol{\psi}_j^S(a, \theta_j) Y_m(z) \right.$$

$$\left. + \left(\mathbf{a}_j^T + \sum_{\substack{i=1 \\ (i \neq j)}}^{N} \mathbf{A}_i^T \mathbf{T}_{ij} \right) \boldsymbol{\psi}_j^I(a, \theta_j) Y_m(z) \right] a \cos \theta_j \, d\theta_j \, dz \quad (m \geq 0) \tag{19}$$

$$a_{zz_j} + i \frac{b_{zz_j}}{\omega} = \rho h \int_{\theta=0}^{2\pi} \int_{r=0}^{a} \left[\left(\mathbf{a}_j^T + \sum_{\substack{i=1 \\ (i \neq j)}}^{N} \mathbf{A}_i^T \mathbf{T}_{ij} \right) \mathbf{B}_{hj}^T \boldsymbol{\psi}_j^S(r_j, \theta_j) \right.$$

$$+ \left(\mathbf{a}_j^T + \sum_{\substack{i=1 \\ (i \neq j)}}^{N} \mathbf{A}_i^T \mathbf{T}_{ij} \right) \boldsymbol{\psi}_j^I(r_j, \theta_j) Y_m(h)$$

$$\left. - \left(\mathbf{a}_j^T + \sum_{\substack{i=1 \\ (i \neq j)}}^{N} \mathbf{A}_i^T \mathbf{T}_{ij} \right) Y_m(h) i^l J_l(k_0 r_j) e^{il\theta_j} \right] r_j \, d\theta_j \, dr_j \tag{20}$$

Pitch added mass and damping coefficients can be calculated in an identical manner to heave and surge.

Most of the literature mentioned in section 1, such as Linton and Evans (1990) and Kim (1992), solves the hydrodynamic interaction problem of bottom-mounted cylinders. Williams and his colleagues tackle the problem for truncated cylinders using the approximate modified plane wave method of McIver and Evans. But the formulations derived in this section to calculate hydrodynamic forces are for truncated circular cylinders, and they are exact within the context of linear theory. Numerical implementation of the equations is quite easy. Once the single body diffraction (radiation) problem is solved, hydrodynamic interaction between the cylinders could be calculated by solving algebraic equations (10) or (16). After that, substituting coefficients A_i in (13) and (15) will give diffraction forces [(19) and (20) will give added mass and damping coefficients].

NUMERICAL RESULTS AND DISCUSSION

Configurations chosen to validate the present method are depicted in Fig. 2. The first geometry is an array of two cylinders; the second one is an array of four cylinders. The distance between the centers of the adjacent cylinders is 2.6 m for geometry (a) and 76 m for geometry (b).

Ninety unknowns, four angular components, and four evanescent modes are used for configuration (a). Dimensions of the cylinders and the water depth in geometry (b) are chosen to be in the same scale as a TLP geometry. For geometry (b), 156 unknowns and 19 angular components are used. However, evanescent modes are not employed for this geometry due to computational difficulties that arise from the larger number of

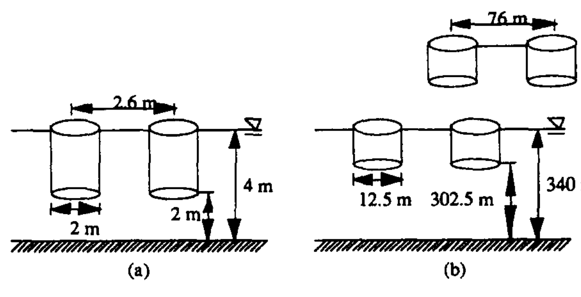

FIG. 2. Configurations Used in Calculations: (a) Two Truncated Cylinders; (b) Four Truncated Cylinders

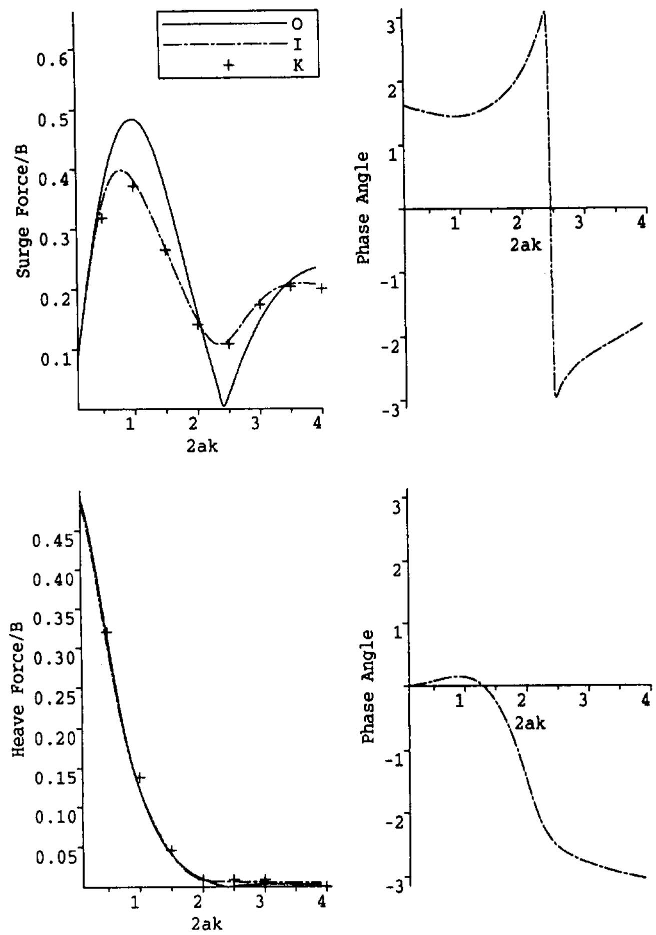

FIG. 3. Results for Two Truncated Cylinders (O = Interaction Based on Incident Wave Phasing; K = Kagemoto's Results; I = Present Method)

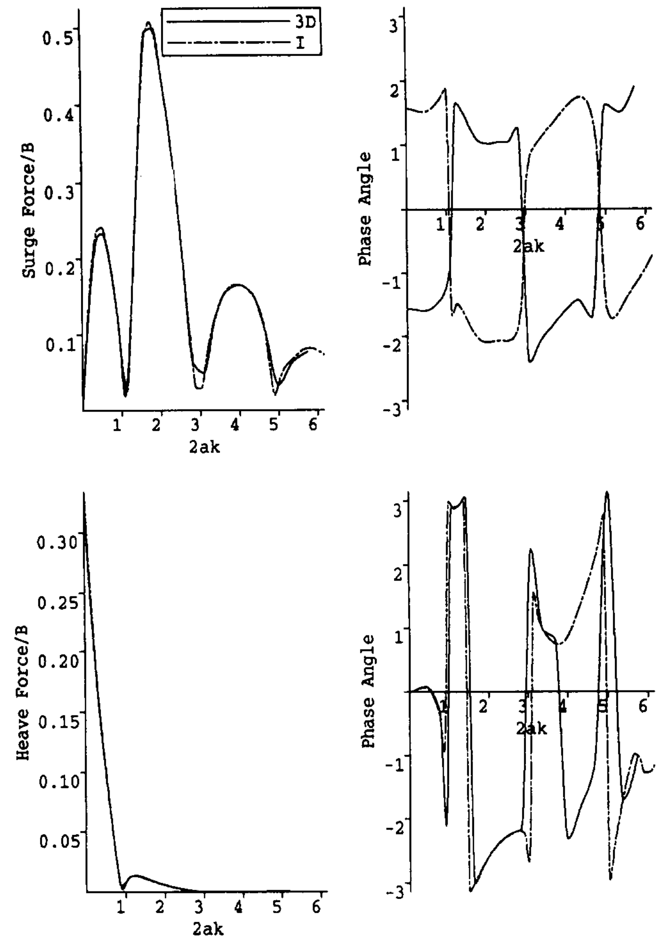

FIG. 4. Results for Four Truncated Cylinders (3D = 3D Program Results; I = Present Method)

unknowns involved in the single body diffraction calculations, compared to geometry (a). Surge and heave forces shown in Figs. 3 and 4 are nondimensionalized by $B = \rho g \pi a(d - h)HN$ and pitch moment in Fig. 5 by $B = \rho g \pi a^2(d - h)HN$. Wave forces and moments are calculated for 0° wave angle of attack. Added mass and damping values shown in Figs. 6 and 7 are nondimensionalized by $A = \rho \pi a^2(d - h)N$ and $A = \omega \rho \pi a^2(d - h)N$, respectively. Surge and heave forces produced for the first geometry are compared with Kagemoto and Yue's results, and the agreement is very good (see Fig. 3). Interaction that uses forces on a single column and incident wave phasing only, denoted by 0 in Fig. 3, produces reasonable results for heave forces. Wave forces and moments and added mass and damping values produced using interaction theory for geometry (b) are compared with the results of a 3D diffraction radiation code based on the 3D source distribution technique developed by Chan (1990) in Figs. 4–7. Chan (1990) made the usual assumptions of a 3D linearized potential theory in deriving the first-order and second-order hydrodynamic forces acting on a body placed in regular, monochromatic waves. In the calculation of forces he used a 3D translating pulsating source model. Chan (1993) extended his method to predict the motion and wave loads of twin hull ships. Agreement between the 3D results and the present method results is very good for surge and heave forces and also for pitch moment (see Figs. 4 and 5). However there are small discrepancies for added mass and damping coefficients in Figs. 6 and 7, especially in the low frequency region of heave added mass and damping (see Fig. 7). These differences can be attributed to the imperfections that exist in the discretization of the bodies. Effect of local waves is not important in this case, since the distance between the cylinders is quite large compared to the diameter (see Kagemoto and Yue 1986).

APPENDIX I.

Scattering of Progressive Incident Waves by Single Truncated Cylinder

The solution given by Garret (1971) is followed. It is a well-known boundary value problem: Fluid motion is governed by Laplace's equation together with the boundary conditions on the free surface, seabed, and body surface and radiation condition at infinity.

$$\nabla^2 \phi = 0 \tag{21}$$

$$\frac{\partial^2 \phi}{\partial t^2} + g \frac{\partial \phi}{\partial z} = 0 \quad \text{on} \quad z = d \tag{22}$$

$$\frac{\partial \phi}{\partial z} = 0 \quad \text{on} \quad z = 0 \tag{23}$$

$$\frac{\partial \phi}{\partial z} = 0 \quad \text{on} \quad z = h, \quad 0 \le r \le a \tag{24}$$

$$\frac{\partial \phi}{\partial r} = 0 \quad \text{on} \quad r = a, \quad h \le z \le d \tag{25}$$

$$\sqrt{r}\left(\frac{\partial \phi}{\partial r} - ik\phi\right) = 0 \quad r \to \infty \tag{26}$$

The fluid domain is divided into two regions, one beneath the cylinder, the interior region (1), the other exterior to the cylinder, exterior region (2) (see Fig. 8).

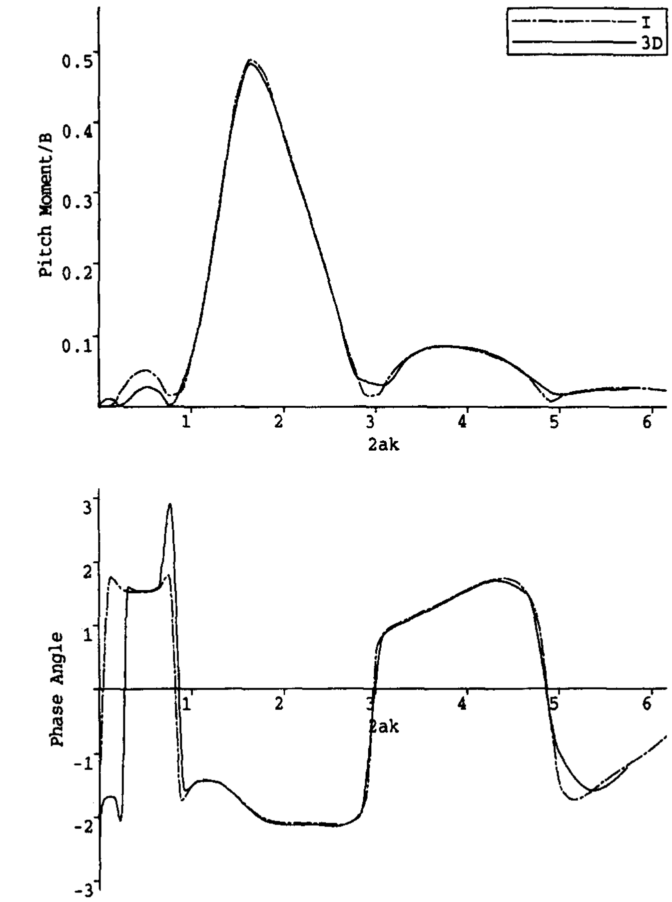

FIG. 5. Results for Four Truncated Cylinders (3D = 3D Program Results; I = Present Method)

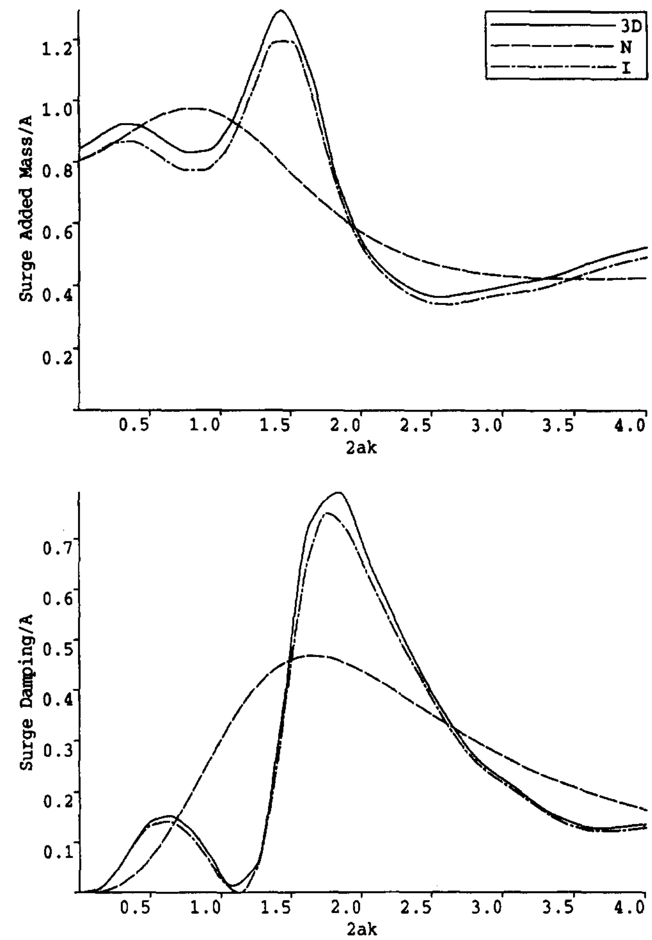

FIG. 6. Results for Four Truncated Cylinders (3D = 3D Program Results; N = No Interaction; I = Present Method)

The incident wave potential is defined as follows:

$$\phi_I = \frac{gH}{\omega}\frac{\cosh k_0 z}{\cosh k_0 d}\sum_{l=-\infty}^{\infty} e^{il[(\pi/2)-\theta]}J_l(k_0 r)e^{-i\omega t} \tag{27}$$

Potential in the interior region that satisfies (21), (23), and (24) is given as follows:

$$\phi_1 = \frac{gH}{\omega}\sum_{l=-\infty}^{\infty}\chi_1^{(l)}(r, z)e^{il\theta}e^{-i\omega t} \tag{28}$$

$$\chi_1^{(l)}(r, z) = \frac{C_0^{(l)}}{2}\left(\frac{r}{a}\right)^{|l|} + \sum_{n=1}^{\infty} C_n^{(l)}\frac{I_l(n\pi r/h)}{I_l(n\pi a/h)}\cos(n\pi z/h) \tag{29}$$

where $C_n^{(l)}$ is given by

$$C_n^{(l)} = \frac{2}{h}\int_{z=0}^{h}\chi_1^{(l)}(a, z)\cos(n\pi z/h)\,dz \tag{30}$$

The exterior potential that consists of incident and diffracted wave fields satisfies (21), (22), (23), and (25) [diffracted waves also satisfy (26)]:

$$\phi_2 = \frac{gH}{\omega}\sum_{l=-\infty}^{\infty}\chi_2^{(l)}(r, z)e^{il\theta}e^{-i\omega t} \tag{31}$$

$$\chi_2^{(l)}(r, z) = i^l\frac{\cosh k_0 z}{\cosh k_0 d}\left\{J_l(k_0 r) - \frac{J_l'(k_0 a)}{H_l^{(1)\prime}(k_0 a)}H_l^{(1)}(k_0 r)\right\} + \sum_{q=0}^{\infty} D_q^{(l)}\frac{V_l(k_q r)}{V_l'(k_q a)}Z_q(z) \tag{32}$$

where

$$V_l(k_0 r) = H_l^{(1)}(k_0 r) \quad \text{for} \quad q = 0 \tag{33a}$$

$$V_l(k_q r) = K_l(k_q r) \quad \text{for} \quad q > 0 \tag{33b}$$

$D_q^{(1)}$ is given by

$$D_q^{(1)} = \frac{1}{k_q d}\int_0^d \frac{\partial\chi_2^{(1)}}{\partial r}(a, z)Z_q(z)\,dz \tag{34}$$

The functions $Z_q(z)$ are orthonormal over the interval $[0, d]$ and are defined by

$$Z_0(z) = \frac{\cosh k_0 z}{N_0^{1/2}} \quad \text{for} \quad q = 0 \tag{35a}$$

$$Z_q(z) = \frac{\cos k_q z}{N_q^{1/2}} \quad \text{for} \quad q > 0 \tag{35b}$$

N_0 and N_q are defined in (12).

The matching conditions, i.e., continuity of mass flux and pressure, should be applied on the interface $r = a$, to determine the coefficients $C_m^{(l)}$ and $D_q^{(1)}$,

$$\chi_1^{(l)} = \chi_2^{(l)} \quad \text{on} \quad r = a, \quad 0 \le z \le h \tag{36a}$$

$$\frac{\partial\chi_1^{(l)}}{\partial r} = \frac{\partial\chi_2^{(l)}}{\partial r} \quad \text{on} \quad r = a, \quad 0 \le z \le h \tag{36b}$$

$$\frac{\partial\chi_2^{(l)}}{\partial r} = 0 \quad \text{on} \quad r = a, \quad h \le z \le d \tag{36c}$$

Applying the matching condition (36*a*) to (30), and (36*b*) and (36*c*) to (34) yields two sets of infinite complex matrix equations

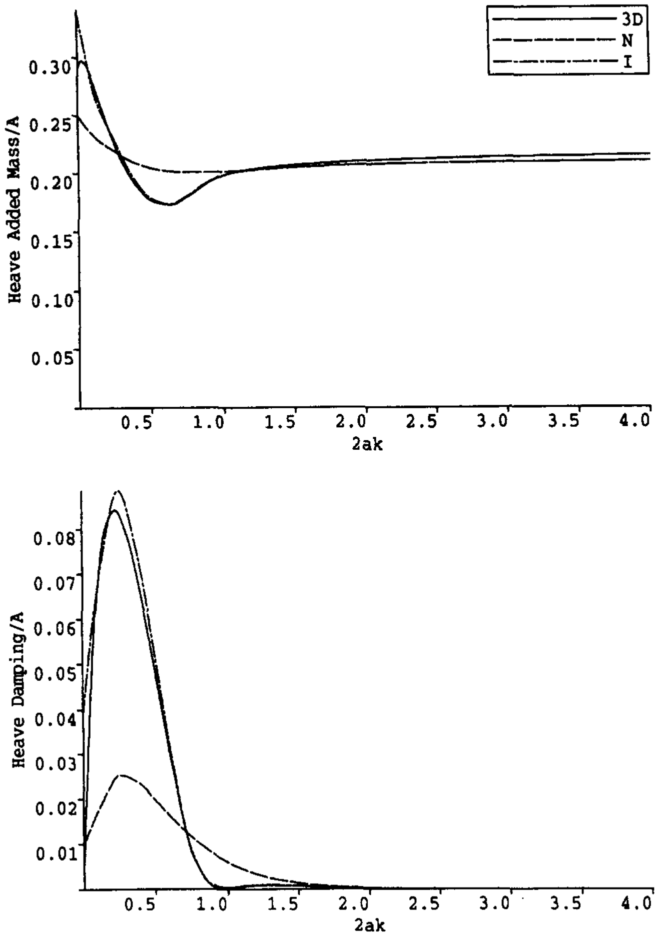

FIG. 7. Results for Four Truncated Cylinders (3D = 3D Program Results; N = No Interaction; I = Present Method)

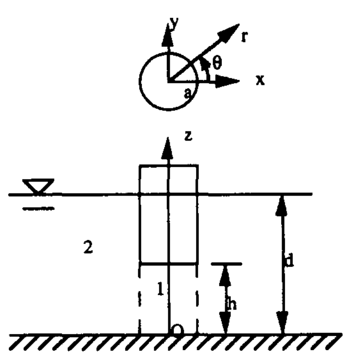

FIG. 8. Definition Sketch for Isolated Cylinder

$$C_n^{(l)} + \sum_{q=0}^{\infty} F_{nq}^{(l)} D_q^{(l)} = R_n^{(l)};\quad D_q^{(l)} = \sum_{n=0}^{\infty} G_{qn}^{(l)} C_n^{(l)} \quad (37a,b)$$

where

$$F_{n0}^{(l)} = -\frac{2}{h}\frac{V_l(k_0a)}{V_l'(k_0a)}\frac{h^2k_0(-1)^n \sinh k_0h}{N_0^{1/2}(n^2\pi^2 + k_0^2h^2)} \quad (n \geq 0) \quad (38a)$$

$$F_{nq}^{(l)} = -\frac{2}{h}\frac{V_l(k_qa)}{V_l'(k_qa)}\frac{h^2k_q(-1)^n \sin k_qh}{N_q^{1/2}(-n^2\pi^2 + k_q^2h^2)} \quad (q \geq 1,\ n \geq 0) \quad (38b)$$

$$G_{00}^{(l)} = \frac{l \sinh k_0h}{2ak_0^2dN_0^{1/2}} \quad (38c)$$

$$G_{q0}^{(l)} = \frac{l \sin k_qk}{2ak_q^2dN_q^{1/2}} \quad (q \geq 1) \quad (38d)$$

$$G_{0n}^{(l)} = \frac{I_l'(n\pi a/h)}{I_l(n\pi a/h)}\frac{n\pi h(-1)^n \sinh k_0h}{(n^2\pi^2 + k_0^2h^2)dN_0^{1/2}} \quad (n \geq 1) \quad (38e)$$

$$G_{qn}^{(l)} = \frac{I_l'(n\pi a/h)}{I_l(n\pi a/h)}\frac{n\pi h(-1)^n \sin k_qh}{(-n^2\pi^2 + k_q^2h^2)dN_q^{1/2}} \quad (q \geq 1,\ n \geq 1) \quad (38f)$$

$$R_n^{(l)} = 2i^l \frac{hk_0(-1)^n \sinh k_0h}{(n^2\pi^2 + k_0^2h^2)\cosh k_0d}\frac{2i}{\pi k_0aH_l^{(1)\prime}(k_0a)} \quad n \geq 0 \quad (38g)$$

These equations may be truncated after a finite number of terms and the coefficients obtained by standard matrix solving techniques. Now the single body diffraction matrices given in (11a) are obtained from (32),

$$\mathbf{B}_j(l) = -\frac{J_l'(k_0a)}{H_l^{(1)\prime}(k_0a)} + \frac{D_0^{(l)}\sqrt{2}\cosh(k_0d)}{H_l^{(1)\prime}(k_0a)\sqrt{1 + \sinh(2k_0d)/(2k_0d)}} \quad (39)$$

$\mathbf{B}_j$ matrices used for the heave force calculations given in (14) are obtained from (29) as follows:

$$B_{hj}(l) = \frac{C_0^{(l)}}{2a^{|l|}} \quad \text{for } n = 0 \quad (40a)$$

$$B_{hj}(n, l) = \frac{C_n^{(l)}}{I_l\left(\frac{n\pi a}{h}\right)}(-1)^n \quad \text{for} \quad n > 0 \quad (40b)$$

Heave force given by the real part of $F_ze^{-i\omega t}$ is derived as follows by integrating the potential around the cylinder:

$$F_z = i\rho gH \int_0^{2\pi}\int_0^a \sum_{l=-\infty}^{\infty} \chi_1^{(l)}(r, z)e^{il\theta}r\,dr\,d\theta \quad (41a)$$

$$F_z = 2i\pi\rho gH\left[\frac{C_0^{(0)}}{2}\frac{a^2}{2} + \sum_{n=1}^{\infty} C_n^{(0)}\frac{I_1(n\pi a/h)}{I_0(n\pi a/h)}\frac{ha}{n\pi}(-1)^n\right] \quad (41b)$$

Surge force given by the real part of $F_xe^{-i\omega t}$ is obtained as follows:

$$F_x = -i\rho gH \int_0^{2\pi}\int_h^d \sum_{l=-\infty}^{\infty} \chi_2^{(l)}(r, z)e^{il\theta}a\,d\theta\,dz \quad (42a)$$

$$F_x = -i\rho gHa\pi\left[\frac{2i(\sinh k_0d - \sinh k_0h)}{k_0\cosh k_0d}\frac{2i}{\pi k_0aH_1^{(1)\prime}(k_0a)} + \sum_{q=0}^{\infty}(D_q^{(-1)} + D_q^{(1)})\frac{V_l(k_qa)}{V_l'(k_qa)}\frac{\gamma(q)}{k_qN_q^{1/2}}\right] \quad (42b)$$

where $\gamma(0) = (\sinh k_0d - \sinh k_0h)$ for $q = 0$; and $\gamma(q) = (\sin k_qd - \sin k_qh)$ for $q > 0$.

Pitch moment about the axis shown in Fig. 8 is given by the real part of $Me^{-i\omega t}$, where M is made up of M_z, arising from forces on the bottom of the dock, and M_x, arising from forces on the side of the dock.

$$M_z = -i\rho gH \int_0^{2\pi}\int_0^a \sum_{l=-\infty}^{\infty} \chi_1^{(l)}(r, z)e^{il\theta}r\,dr\,d\theta r\cos\theta \quad (43a)$$

$$M_z = -i\pi\rho gH\left[\frac{(C_0^{(-1)} + C_0^{(1)})}{2a}\frac{a^4}{4} + \sum_{n=1}^{\infty}(C_n^{(-1)} + C_n^{(1)})\frac{I_2(n\pi a/h)}{I_1(n\pi a/h)}\frac{ha^2}{n\pi}(-1)^n\right] \quad (43b)$$

$$M_x = -i\rho gH \int_0^{2\pi}\int_h^d \sum_{l=-\infty}^{\infty} \chi_2^{(l)}(r, z)e^{il\theta}a\,d\theta\,dz(d - z) \quad (44a)$$

$$M_x = -i\pi\rho gHa\left[\frac{2i}{\cosh k_0 d} \frac{2i\lambda(0)}{\pi k_0 a H_1^{(1)'}(k_0 a)} + \sum_{q=0}^{\infty} (D_q^{(-1)} + D_q^{(1)}) \frac{V_1(k_q a)}{V_1'(k_q a)} \frac{\lambda(q)}{N_q^{1/2}}\right] \quad (44b)$$

where

$$\lambda(0) = \frac{(h-d)\sinh k_0 h}{k_0} + \frac{\cosh k_0 d - \cosh k_0 h}{k_0^2} \quad \text{for} \quad q = 0$$

$$\lambda(q) = \frac{(h-d)\sin k_q h}{k_q} + \frac{\cos k_q h - \cos k_q d}{k_q^2} \quad \text{for} \quad q \ge 0$$

Scattering of Evanescent Incident Waves by Single Truncated Cylinder

Evanescent incident wave potential is given by

$$\phi_I = \frac{gH}{\omega} \cos k_m z \sum_{l=-\infty}^{\infty} e^{il\theta} I_l(k_m r) e^{-i\omega t}; \quad m = 1, 2, \ldots \quad (45)$$

Evanescent mode solution is similar to the progressive mode, only the exterior region potential will be different:

$$\chi_2^{(l)}(r, z) = \cos k_m z \left[I_l(k_m r) - \frac{I_l'(k_m a)}{K_l'(k_m a)} K_l(k_m r) \right] + \sum_{q=0}^{\infty} D_q^{(l)} \frac{V_l(k_q r)}{V_l'(k_q a)} Z_q(z); \quad n = 1, 2, \ldots \quad (46)$$

Matching conditions and the solution procedure are identical to the progressive mode. $\mathbf{B}_j$ matrices used for the interaction theory given by (11*b*) are derived from the foregoing expression as follows:

$$\mathbf{B}_j(m, q, l) = -\frac{I_l'(k_m a)}{K_l'(k_m a)} + \frac{D_m^{(l)}}{K_l'(k_m a) N_m^{1/2}} \quad (47)$$

APPENDIX II.

Radiation Problem of Single Truncated Cylinder in Heave Mode

Presentation of the problem and the solution is very similar to the diffraction problem: the governing equation is Laplace's equation together with the boundary conditions at the free surface, body surface, and seabed and radiation condition at infinity. However, body boundary conditions are different and (24) and (25) should be modified as follows:

$$\frac{\partial \phi}{\partial z} = V_z \quad \text{on} \quad z = h, \quad 0 \le r \le a \quad (48)$$

$$\frac{\partial \phi}{\partial r} = 0 \quad \text{on} \quad r = a, \quad h \le z \le d \quad (49)$$

The fluid domain is divided into two regions, one beneath the cylinder, the interior region (1), the other exterior to the cylinder, exterior region (2) (see Fig. 8).

Potential in the interior region that satisfies (21), (23), and (48) is given as follows:

$$\phi_1 = V_z h \zeta_1(r, z) e^{-i\omega t} \quad (50)$$

$$\zeta_1(r, z) = \Lambda_{1h}(r, z) + \Lambda_{1p}(r, z) \quad (51)$$

where $\Lambda_{1p}(r, z)$ = particular solution that satisfies (21), (23), and (48) and is given by

$$\Lambda_{1p}(r, z) = \frac{1}{2hd}(z^2 - r^2/2) \quad (52)$$

$\Lambda_{1h}(r, z)$ is the homogeneous solution and is given by

$$\Lambda_{1h}(r, z) = \frac{C_0}{2} + \sum_{n=1}^{\infty} C_n \frac{I_0(n\pi r/h)}{I_0(n\pi a/h)} \cos(n\pi z/h) \quad (53)$$

where C_n is given by

$$C_n = \frac{2}{h} \int_{z=0}^{h} \Lambda_{1h}(a, z) \cos(n\pi z/h)\, dz \quad (54)$$

The exterior potential satisfies equations (21), (22), (23), (26), and (49):

$$\phi_2 = V_z h \zeta_2(r, z) e^{-i\omega t} \quad (55)$$

$$\zeta_2(r, z) = \sum_{q=0}^{\infty} D_q \frac{V_0(k_q r)}{V_0'(k_q a)} Z_q(z) \quad (56)$$

where $D_q^{(1)}$ is given by

$$D_q = \frac{1}{k_q d} \int_0^d \frac{\partial \zeta_2}{\partial r}(a, z) Z_q(z)\, dz \quad (57)$$

The matching conditions, i.e., continuity of mass flux and pressure, should be applied on the interface $r = a$, to determine the coefficients $C_m^{(l)}$ and $D_q^{(1)}$,

$$\zeta_1 = \zeta_2 \quad \text{on} \quad r = a, \quad 0 \le z \le h \quad (58a)$$

$$\frac{\partial \zeta_1}{\partial r} = \frac{\partial \zeta_2}{\partial r} \quad \text{on} \quad r = a, \quad 0 \le z \le h \quad (58b)$$

$$\frac{\partial \zeta_2}{\partial r} = 0 \quad \text{on} \quad r = a, \quad h \le z \le d \quad (58c)$$

By applying (58*a*) to (54) and (58*b*) and (58*c*) to (57), one obtains two sets of infinite complex matrix equations

$$C_n + \sum_{q=0}^{\infty} F_{nq} D_q = R_n; \quad D_q = \sum_{n=0}^{\infty} G_{qn} C_n + S_q \quad (59a,b)$$

where F_{nq} and G_{qn} are given in (38*a*)–(38*f*) with l being zero. R_n and S_q are given as follows:

$$R_0 = -\frac{1}{3} + \frac{a^2}{2h^2} \quad n = 0; \quad R_n = -\frac{2(-1)^n}{(n\pi)^2} \quad n > 0 \quad (60a,b)$$

$$S_0 = -\frac{a}{2h^2} \frac{\sinh k_0 h}{k_0^2 d N_0^{1/2}} \quad q = 0; \quad S_q = -\frac{a}{2h^2} \frac{\sin k_q h}{k_q^2 d N_q^{1/2}} \quad q > 0 \quad (61a,b)$$

Heave added mass and damping are obtained by integrating the interior region potential over the cylinder bottom,

$$a_{zz} + i\frac{b_{zz}}{\omega} = \rho h \int_0^{2\pi} \int_0^a \zeta_1(r, z) r\, dr\, d\theta \quad (62a)$$

$$a_{zz} + i\frac{b_{zz}}{\omega} = 2\pi\rho h \left[\frac{a^2}{4} - \frac{a^4}{16h^2} + C_0 \frac{a^2}{4} + \sum_{n=1}^{\infty} C_n \frac{I_1(n\pi a/h)}{I_0(n\pi a/h)} \frac{ha}{n\pi} (-1)^n\right] \quad (62b)$$

Radiation Problem of Single Truncated Cylinder in Surge Mode

Presentation of the problem and the solution is similar to the heave problem. Only body boundary conditions are different, therefore (48) and (49) should be modified as follows:

$$\frac{\partial \phi}{\partial z} = 0 \quad \text{on} \quad z = h, \quad 0 \le r \le a \quad (63)$$

$$\frac{\partial \phi}{\partial r} = V_x \cos\theta \quad \text{on} \quad r = a, \quad h \le z \le d \quad (64)$$

Potential in the interior region is given as follows:

$$\phi_1 = V_x d\zeta_1(r, z)\cos\theta e^{-i\omega t} \tag{65}$$

$$\zeta_1(r, z) = \Lambda_{1h}(r, z) + \Lambda_{1p}(r, z) \tag{66}$$

The particular solution, $\Lambda_{1p}(r, z)$ is equal to zero. The homogeneous part of the interior potential is given by the following equation:

$$\Lambda_{1h}(r, z) = \frac{C_0}{2}\left(\frac{r}{a}\right) + \sum_{n=1}^{\infty} C_n \frac{I_1(n\pi r/h)}{I_1(n\pi a/h)}\cos(n\pi z/h) \tag{67}$$

The exterior potential is given as follows:

$$\phi_2 = V_x d\zeta_2(r, z)\cos\theta e^{-i\omega t} \tag{68}$$

where $\zeta_2(r, z)$ is given by (56) with the order of Bessel function being 1 instead of 0.

The matching conditions (58*a*) and (58*b*) still hold; however, (58*c*) should be modified as follows:

$$\frac{\partial\zeta_2}{\partial r} = 1 \quad \text{on} \quad r = a, \quad h \le z \le d \tag{69}$$

There are also changes to the coefficients of the two sets of infinite complex matrix equations given in (59*a*) and (59*b*). F_{nq} and G_{qn} are given in (38*a*)–(38*f*) with l being one. R_n is equal to zero since the particular solution is zero. S_q is given as follows:

$$S_q = \frac{\gamma(q)}{k_q^2 d^2 N_q^{1/2}} \quad n \ge 0 \tag{70}$$

where $\gamma(q)$ is as described in (42).

Surge added mass and damping are obtained by integrating the interior region potential over the cylinder surface,

$$a_{xx} + i\frac{b_{xx}}{\omega} = -\rho d \int_0^{2\pi}\int_0^a \zeta_2(r, z)\cos\theta a\, d\theta\, dz \cos\theta$$

$$= -\pi\rho a d\left[\sum_{q=0}^{\infty} D_q \frac{V_1(k_q a)}{V_1'(k_q a)}\frac{\gamma(q)}{k_q N_q^{1/2}}\right] \tag{71}$$

ACKNOWLEDGMENTS

The study reported here was carried out with financial support from the University of Glasgow. The permission of the Technical University of Istanbul for the writer to take a leave of absence in order to carry out this study is also gratefully acknowledged.

APPENDIX III. REFERENCES

Abramowitz, M., and Stegun, I. A. (1964). *Handbook of mathematical functions.* Government Printing Office, Washington, D.C.

Chan, H. S. (1990). "A three-dimensional technique for predicting first- and second-order hydrodynamic forces on a marine vehicle advancing in waves," PhD thesis, Dept. of Naval Arch. and Oc. Engrg., Univ. of Glasgow, Glasgow, U.K.

Chan, H. S. (1993). "Prediction of motion and wave loads of twin-hull ships." *Marine Struct.*, 6, 75–102.

Garret, C. J. R. (1971). "Wave forces on a circular dock." *J. Fluid Mech.*, Cambridge, U.K., 46, 129–139.

Kagemoto, H., and Yue, D. K. P. (1986). "Interactions among multiple three-dimensional bodies in water waves: An exact algebraic method." *J. Fluid Mech.*, Cambridge, U.K., 166, 189–209.

Kim, M. H. (1992). "Interaction of waves with N vertical circular cylinders." *J. Wtrwy., Port, Coast., and Oc. Engrg.*, ASCE, 119(6), 671–689.

Linton, C. M., and Evans, D. V. (1990). "The interaction of waves with arrays of vertical circular cylinders." *J. Fluid Mech.*, Cambridge, U.K., 46, 549–569.

McIver, P. (1984). "Wave forces on arrays of floating bodies." *J. Engrg. Mathematics*, 18, 273–285.

McIver, P., and Evans, D. V. (1984). "Approximation of wave forces on cylinder arrays." *Appl. Oc. Res.*, 6, 101–107.

Ohkusu, M. (1974). "Hydrodynamic forces on multiple cylinders in waves." *Proc., Int. Symp. on Dyn. of Marine Vehicles and Struct. in Waves*, Paper 12, London, U.K., 107–112.

Simon, M. J. (1982). "Multiple scattering in arrays of axisymmetric wave-energy devices. Part 1. A matrix method using a plane-wave approximation." *J. Fluid Mech.*, Cambridge, U.K., 120, 1–125.

Spring, B. H., and Monkmeyer, P. L. (1974). "Interaction of plane waves with vertical cylinders." *Proc., 14th Int. Conf. on Coast. Engrg.*, ASCE, New York, N.Y., 1828–1845.

Williams, A. N., and Abul-Azm, A. G. (1989). "Hydrodynamic interactions in floating cylinder arrays. II: Wave radiation." *Oc. Engrg.*, 16(3), 217–263.

Williams, A. N., and Demirbilek, Z. (1988). "Hydrodynamic interactions in floating cylinder arrays. II: Wave scattering." *Oc. Engrg.*, 15(6), 549–583.

Williams, A. N., and Rangappa, T. (1994). "Approximate hydrodynamic analysis of multi-column ocean structures." *Oc. Engrg.*, 21(6), 519–573.